Influence of data source and copula statistics on estimates of compound **flood** extreme~~s water levels~~ in a river mouth environment

Kévin Dubois[1,2], Morten Andreas Dahl Larsen[3,4], Martin Drews[3], Erik Nilsson[1,2], Anna Rutgersson[1,2]

[1]Department of Earth Sciences, Uppsala University, Uppsala, 752 36, Sweden
[2]Centre of Natural Hazards and Disaster Science (CNDS), Uppsala University, Uppsala, 752 36, Sweden
[3]Department of Technology, Management and Economics, Technical University of Denmark, Lyngby, 2800, Denmark
[4]Danish Meteorological Office, Copenhagen, 2100, Denmark

Correspondence to: Kévin Dubois (kevin.dubois@geo.uu.se)

Abstract.

Coastal and riverine floods are major concerns worldwide as they can impact highly populated areas and result in significant economic losses. In a river mouth environment, interacting hydrological and oceanographical processes can enhance the severity of floods. The compound flood risks from high sea levels and high river runoff levels are often indirectly estimated using ~~statistical~~ copulas among other methods. Here, we systematically investigate the influence of different data sources coming from observations and models ~~and~~ as well as the choice of ~~statistical~~ copula on extreme water level estimates. While we focus on the river mouth at Halmstad city (Sweden), the approach presented is easily transferable to other sites. Our results show that the compound occurrence of high sea levels and river runoff may lead to heightened flood risks as opposed to considering them as independent processes and that in the current study, this is dominated by the hydrological driver. We also show that the choice of data sources can considerably impact the results up to 10% and 15% for the river time series and 3% to 4.6% for the sea level time series under the 5- and 30-year return periods respectively. ~~and~~ The choice of copula can also strongly influence the outcome of such analyses up to 13% and 9.5% for the 5-year and 30-year return periods. The copulas found to statistically best fit our datasets are the Clayton, BB1 and Gaussian (once) ones. Our findings contribute to framing existing studies, which typically only consider selected copulas and data sets, by demonstrating the importance of considering uncertainties.

1 Introduction

Floods can cause severe damage and disrupt activities and infrastructures in harbours and coastal communities. Flooding can result from meteorological, hydrological and oceanographic sources such as storm surges, extreme river runoff or precipitation. Storm surges correspond to seawater being pushed by the wind stress and the barometric pressure effect under deep low-pressure weather systems. Heavy precipitation can form under different conditions such as intense cyclonic activity, sometimes during the same deep low-pressure systems that cause the storm surge, or sometimes in ~~or~~ convective weather conditions. River runoff can also have different origins, such as snow melting upstream or intense precipitation, either related

to the same large-scale weather system that could cause the storm surge or separately. Hence, several processes could contribute to compound effects, but also independently cause damage and disruption to activities in the coastal zone. River runoff and precipitation may take some time to drain into the sea, and the flow from land to the sea can therefore be slowed down or even momentarily become blocked when storm surges happen (Wahl et al., 2015). This process can be referred as coastal backwater effects while the water level at the river mouth increases due to high river discharge or high sea level or compounding effects (Feng et al., 2022).

Settlements and infrastructure located in river mouth environments are inherently susceptible to all of the above. The combination of multiple factors, extreme or not, happening at the same place simultaneously, successively, or consecutively, can potentially lead to larger, compounded floods, and more severe impacts on the environment and society. Compound flooding can also result when preceding conditions amplify the impact of the event (Andrée et al., 2023; Zscheischler et al., 2020; AghaKouchak et al., 2020). Even if trends over the last forty to sixty years are estimated with high uncertainties, it is likely that extremes including compound events are becoming more severe in Northern Europe in a changing climate (Rutgersson et al., 2021).

Couasnon et al. (2020) highlight the importance of considering interactions referred to their co-occurrence probabilities between river discharge and storm surge extremes in river mouth environments. They demonstrate that dependencies between these factors drivers are not random and may result from relations between weather systems at the synoptic scale with local conditions such as the topography. Ward et al. (2018) study the dependence between river discharge and skew surge at the global scale where significant dependency is found in several stations in Europe, mainly located around the UK coastline. Hendry et al. (2019) also highlighted those dependencies around the UK coast and linked the spatial variability found with differences in storm characteristics. In Northwestern Europe, it has been shown that the fluvial flood hazard increases with high sea levels and stronger storms, and that this may be critical in populated and low-elevation coastal areas (Ganguli et al., 2019). For example, Eilander et al. (2020) find the Baltic Sea and the Kattegat basin to be particularly susceptible to compound flood hazards based on the dependency between skew surge levels and river discharge. Without considering the occurrence of storm surges, Eilander et al. (2020) further show that flood depths are underestimated and subsequently so is the estimated number of people exposed to river floods in this area. Meanwhile, Moftakhari et al. (2017) demonstrate that sea level rise (SLR) is likely to increase the impacts from compound flooding by 2030 and 2050 under the Representative Concentration Pathways (RCPs) 4.5 and 8.5 for eight major cities around the US coastline.

Compound flooding in coastal areas can also be caused by a combination of heavy precipitation inducing large runoff and high sea levels (Bevacqua et al., 2019). Hence, the probability of compound flooding is expected to significantly increase in the Baltic and North Sea areas, where an event with a current return period (RP) of around sixty years is projected to occur every ten years in 2100 due to the combination of SLR and increased extreme precipitation (Bevacqua et al., 2019).

Not taking compound flooding effects into account may result in an underestimation of the flood hazards in the coastal zone, including river mouths (Ward et al., 2018). Thus, analyzing and understanding these events is of high relevance to coastal communities. In this study, we evaluate the potential impact of extreme hydrological and oceanographic coastal events on the

coastal city of Halmstad (Sweden), which is a port, industrial, and recreational city at the mouth of the Nissan river. Halmstad is located on the west coast of Sweden (fig. 1) and has been chosen as it is naturally prone to coastal, fluvial, and pluvial flooding. The area is subject to extratropical cyclones (Hoskins and Hodges, 2002; Dacre et al., 2012), resulting in rather high sea levels by storm surges for the area (Wolski et al., 2014). According to the Swedish Meteorological and Hydrological Institute (SMHI), Halmstad recorded the highest ever sea level measured in Sweden of 235 cm on the 29th of November 2015 during the wind storm "Gorm". Halmstad has also been severely impacted by river floods. While Nissan is the main river crossing the city of Halmstad, smaller rivers are also present and can create floods, such as Fylleån's river. Finally, the West Coast of Sweden is found to be one of the areas in Sweden expecting the most significant impacts due to SLR during this century (Hieronymus et al.and Kalén, 2020). Thus, nearby studies have stressed the necessity to update coastal protection measures along the Swedish (Hieronymus et al.and Kalén, 2022) and the German Baltic Sea shorelines (Kiesel et al., 2023). To help guiding and communicating with the local municipalities about their continued work to protect coastal areas from flooding we considered it useful to pick one site in this area as an example to showcase the applied methods and their results.

The main goal of the current study is to investigate the impact of different data sources, methodology, and representation of compound extremes on estimates of extreme water levels. Using Halmstad as an example, we explore the potential influence on flood risk assessments related to compound effects from river flooding within the coastal area.
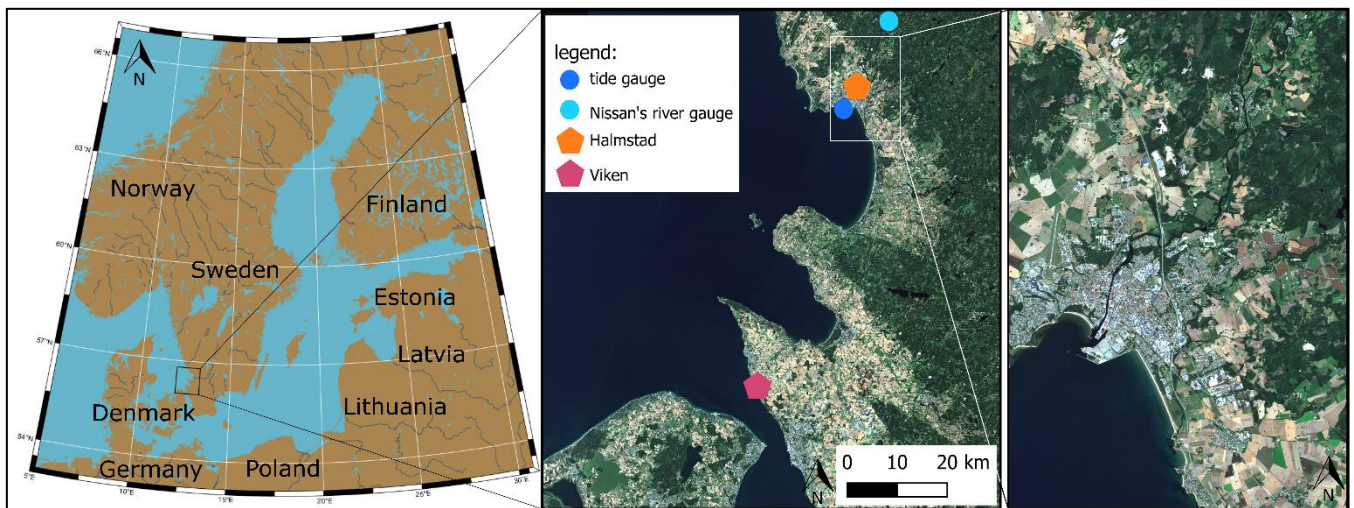
Figure 1: Regional map of southern and central Sweden with a zoom around our study area and the city of Halmstad (Pawlowicz, 2020; Sentinel 2 cloudless, 2021)

2 Data and Methods

In the following, compound effects are defined in terms of the co-occurrence probabilities interaction between coastal sea level and river discharge when at least one of the two is subject to an "extreme" value. An event is considered in the

extreme range when a studied variable reaches its annual maximum value. The annual maximum values will differ between different years in a range between 84 to 235 cm for sea level and 88 to 271 m^3 s^{-1} for river discharge. The correlation between co-occurring events has been studied as it provides insight into the relationship between each set of two variables. The

90 exceedance probability of getting an extreme river discharge associated with a high sea level and the opposite permits the assessment of the potential compound effects between those two processes but it does not determine impacts from compound flooding either in terms of estimating water level or computing inundation depths. Hybrid statistical-hydraulic modeling frameworks have been introduced to answer such issue and study compound flood impacts (Jane et al., 2022; Moftakhari et al., 2019; Gori et al., 2020; Olbert et al., 2023).

95 Figure 2 presents the main steps of the workflow describing the methodology; this is described in the following sub-sections. Firstly, we analyzed different time-series records of sea level and Nissan River discharge data from models and observations at Halmstad using extreme value theory and a Generalized Extreme Value (GEV) distribution (Coles, 2001) – hereby referred to as the "univariate approach" - to estimate Return Levels (RLs) on every factor driver independently. Secondly, we defined sets of coupled events based on single variables. Thirdly, we analyzed the correlation between sea level and river discharge

100 events. If this analysis indicated a potential for compound events, we studied the co-dependency between the two variables by fitting a statistical copula distribution function (Sadegh et al., 2018). We finally performed a statistical analysis of the compound events to study the differences between each data source and its associated uncertainties.
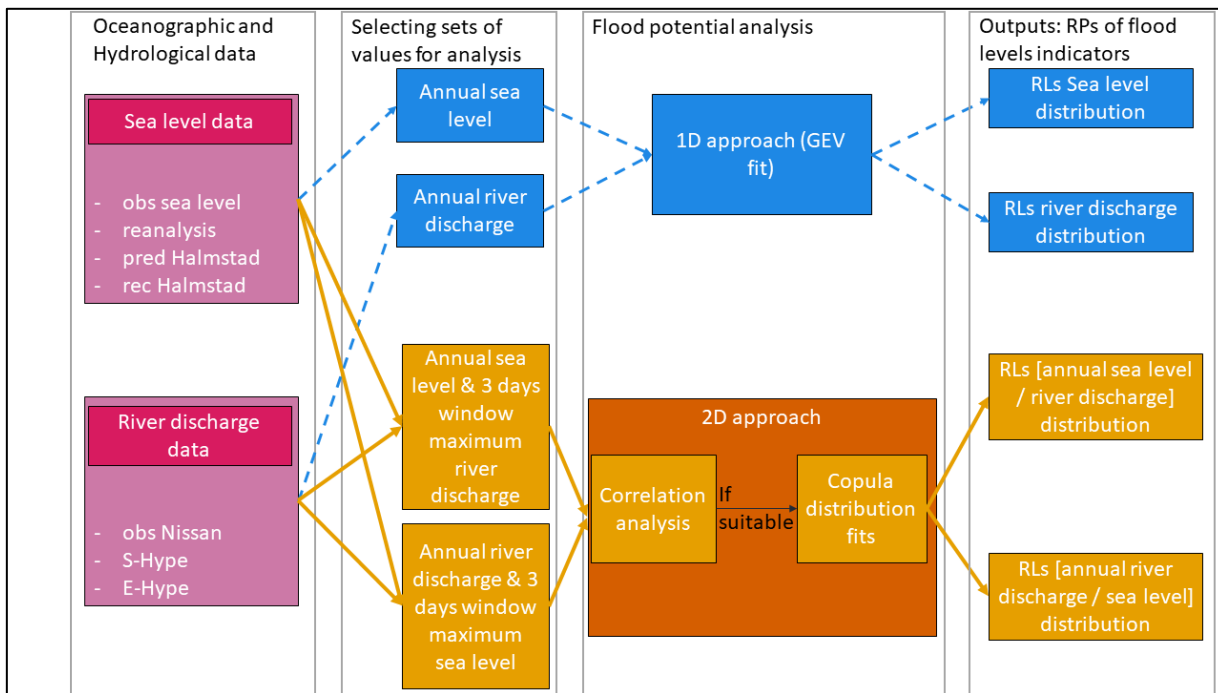
Figure 2: Workflow describing the methodology used in this paper, starting from the oceanographic and hydrological data (in orangepurple) to the univariate (in blue and dashed arrows) and bivariate (in greenorange) approaches used for flood risk analysis.

2.1 Data

An analysis of time-series records of sea level ~~(fig. 3-a)~~ and river discharge ~~(fig. 4-a)~~ at Halmstad was carried out. As mentioned above, a univariate distribution was initially fitted based on the GEV distribution and extreme value theory (Coles, 2001) for each time series collected. The temporal differences in the lengths of each dataset induce substantial differences and associated uncertainties, which dominate in the case of extreme RP. Consequently, a moderately extreme 30-year RP event was chosen as the maximum value considered. For comparison, we also consider more frequent events with a 5-year RP.

2.1.1 Sea level data

Figure 3 displays the different sea level datasets used (fig. 3-a) and their corresponding univariate extreme value analysis (fig. 3-b).
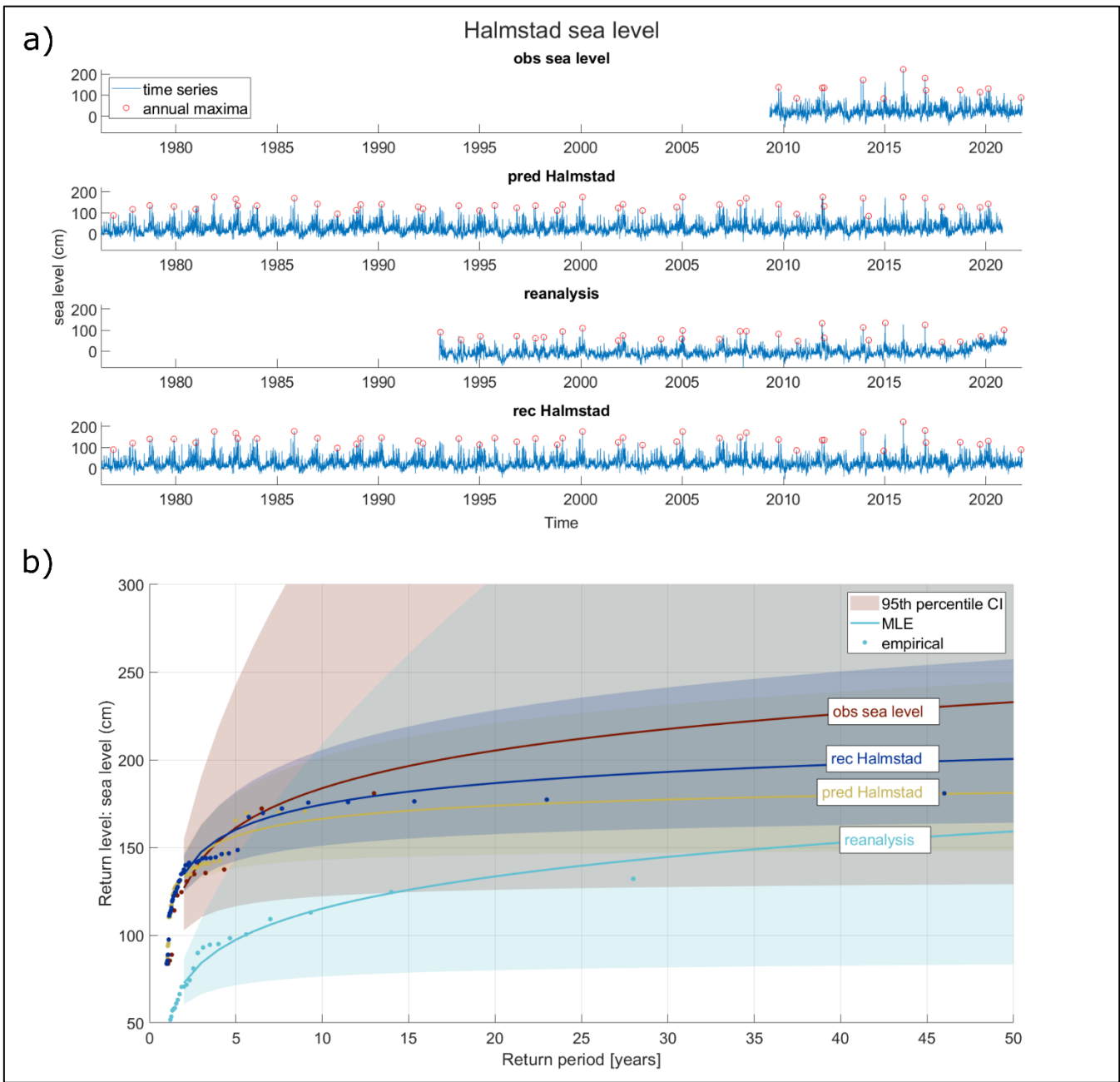
Figure 3: Halmstad sea level time series and annual maxima from different sources: observations ("obs sea level"), reconstructed ("rec Halmstad") and predicted ("pred Halmstad") derived from a machine learning model trained on data from the Viken station, and reanalysis ("reanalysis") datasets (panel a). RLs estimated from corresponding GEV fits of each dataset and the associated 95th percentile confidence intervals (background colours). The dots depict empirical data (panel b).

- ***Observations***

Hourly sea level observations data were obtained from SMHI at Halmstad's tide gauge denoted as the station "HALMSTAD
SJÖV" with station number 35115 in the open database provided by SMHI (fig. 1). This hourly sea level time series is
transformed to a daily time series using the maximum hourly data within the day. However, to carry out this analysis, the
period with sea level observations (titled "obs sea level") was insufficient as only 13 years (from 2009 to 2021) are available;
based on the p-value from correlation analysis the associated results are not statistically insignificant. To extend this sea level
record, a set of reanalysis data and a machine learning approach have been investigated and used.

- ***Reanalysis***

Hourly sea surface variations (in m) covering the period from 1993 to 2020 with a spatial resolution of approximately two
nautical miles have been provided by the Copernicus Marine Environment Monitoring Service's (CMEMS) Baltic Monitoring
and Forecasting Centre (BAL MFC) (CMEMS, 2022). This reanalysis uses the ice-ocean model NEMO-NORDIC (Pemberton
et al., 2017), and the data are assimilated with the Localized Singular Evolutive Interpolated Kalman (LSEIK) method (Nerger
et al., 2005). Data is extracted from the closest grid point to Halmstad's tide gauge and the hourly data was changed to a time
series of daily maxima for our purpose to focus on extremes. This sea level dataset is named: "reanalysis".

- ***Machine learning model***

A probabilistic machine learning method, ~~Quantile Regression~~ Random Forest~~s~~ (~~Q~~RF), is used (~~Meinshausen~~Breiman,
~~2006~~2001). Sea level records from the neighbouring station of Viken (station named "VIKEN", number 2228 in the SMHI
database) is used to train the ~~Q~~RF model over an eight year-period, where it is correlated with Halmstad's observed sea level.
The resulting sea level estimates at Halmstad include both mean predictions and ~~percentiles~~ standard deviation to assess
uncertainties and variability following the methodology introduced by Dubois et al. (202~~4~~3). The last three years of available
data at Halmstad are used to validate the ~~Q~~RF model, emphasizing extreme events predictions. The ~~Q~~RF model is used to
produce a first dataset called: "predicted Halmstad" ("pred Halmstad") and a second one named: "reconstructed Halmstad"
("rec Halmstad").

The predicted Halmstad dataset provides daily sea level (in cm) for the full period of available sea level observations from the
station at Viken, here from 1977 to 2021.

The reconstructed Halmstad dataset provides daily sea level (in cm). It joins both sets, i.e., combines observations
from Halmstad from 2009 to 2021 and the predicted Halmstad data from the ~~Q~~RF model from 1977 to 2009. Thus, it also
covers the period from 1977 to 2021. Further attempts to enrich the ~~Q~~RF model by including reanalysis data (i.e., as part of
the training) did not improve the predicted sea levels in the reconstructed data sets significantly, which emphasized the need
for local observations. These were fortunately available, even if not for the entire more extended period. Similar findings, that

155 is, significant improvements when using local observations as means to train a machine learning of sea level were previously found in this region (e.g. Hieronymus et al., 2019).

It is not only the length of the observation period that is short. Also, the reanalysis dataset exhibits a bias and does 160 not predict the observed extreme sea levels. Accordingly, the uncertainty estimated from both univariate GEV analyses are large (fig. 3-b). The predicted and reconstructed data sets yields result with a smaller uncertainty range. Hence, the reconstructed data set, which is based on observations when available, was chosen as the best source of sea level information for the bivariate analysis.

2.1.2 River runoff data

165 Figure 4 presents the different river discharge datasets obtained (fig. 4-a) and their corresponding univariate extreme value analysis (fig. 4-b).

- ***Observations***

River discharge data were obtained from SMHI at station 2471: "Nissaström" (fig. 1), covering a basin of 2437 km^2. 170 Observations of daily river discharge in ~~m³/s~~$m^3 s^{-1}$ (obs Nissan) have been provided from 1997 to 2021.

- ***E-Hype model***

Modelled river discharge data are taken from the Hydrological Predictions for the Environment (HYPE) model, which simulates water flows and quality at different spatial scales (Lindström et al., 2010), a model detailed description can be found 175 at http://www.smhi.net/hype/wiki/doku.php?id=start. Daily temperature and precipitation values are used as dynamic forcing in this model. The European HYPE model: "E-Hype2016_version_16_g" (E-Hype) provides daily river discharge (in $m^3 s^{-1}$~~m³/s~~) from 1989 to 2021 (https://vattenwebb.smhi.se/om-vattenwebb). The model best performs for annual and seasonal flows compared with daily and extreme flows (Donnelly et al., 2016).

180 - ***S-Hype model***

SMHI has set up the HYPE model for Sweden, now used operationally to forecast hydrological conditions over Sweden, such as floods and droughts. It covers all of Sweden (450000 km^2), where the country has been divided into sub-basins of 28 km^2 on average (Strömqvist et al., 2012). S-Hype3 model's data (S-Hype) of daily river discharge (in $m^3 s^{-1}$~~m³/s~~) has been provided from 2004 to 2020 (Donnelly et al., 2016). The model seems to slightly underestimate high flow peaks with high flow statistics 185 differing by around +-10% whereas the mean flow is highly reliable (Bergstrand et al., 2014).
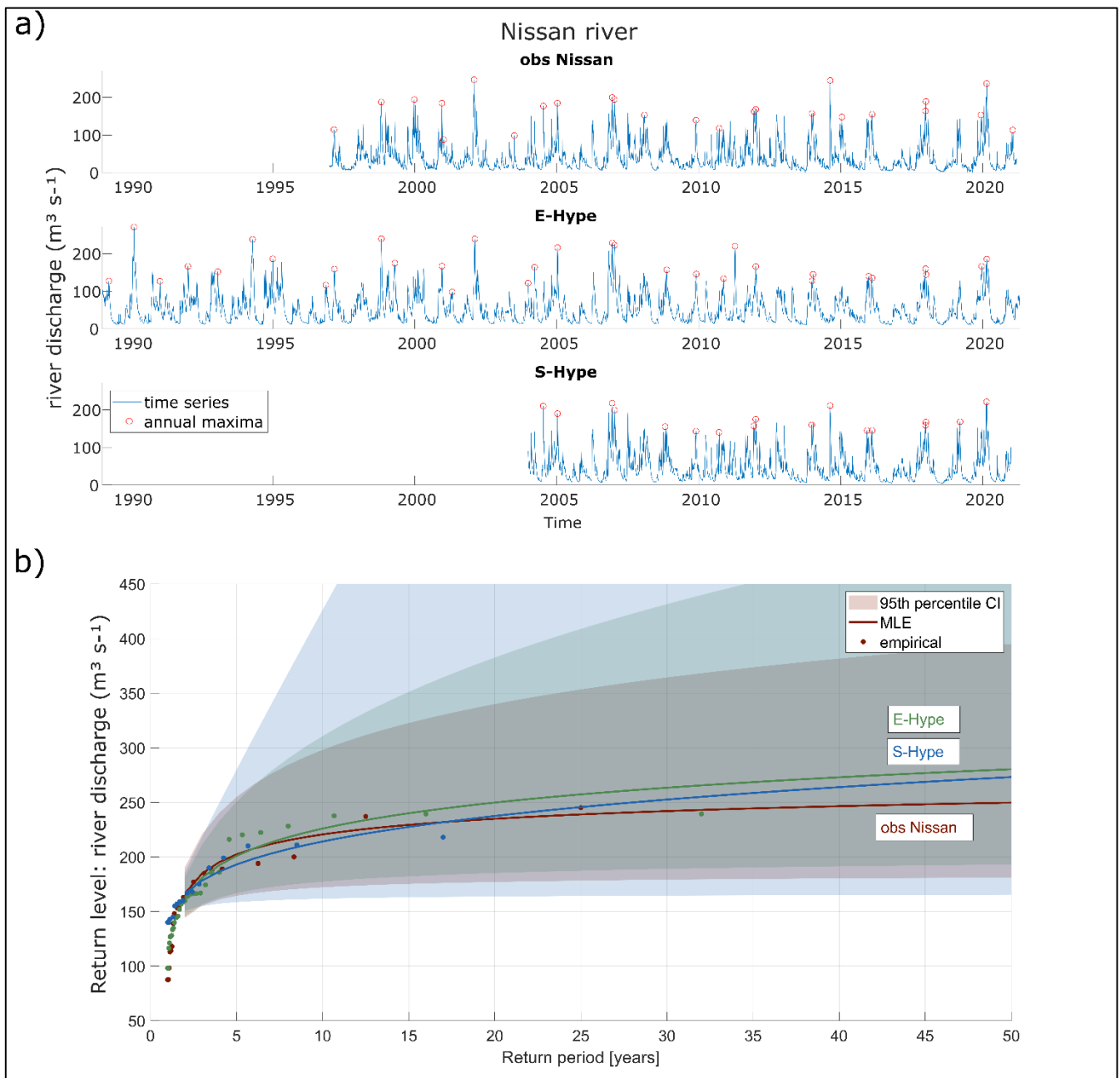
Figure 4: Nissan's river time series and annual maxima from different sources: observations ("obs Nissan"), European HYPE model ("E-Hype") and Swedish HYPE model ("S-Hype") from SMHI (panel a). RLs derived from GEV fits to each dataset are shown with

190 **95th percentile confidence intervals (background colours). The dots are the empirical data (panel b).**

The available time series associated with the S-Hype model is rather limited, leading to a wide uncertainty band when carrying out the univariate analysis (fig. 4). Conversely, the Nissan observations and E-Hype data sets lead to RLs that are associated

with more bounded uncertainty estimates. In this light, we choose the E-Hype dataset for the bivariate analyses as the data are
available over a more extended period. The largest RLs are seen for the E-Hype dataset for RPs above five years.

2.1.3 Sets of coupled events

To study compound events in a river mouth environment from both a river discharge and sea level perspective, we defined two different sets of events based on the data discussed above. The first one ~~used~~ paired sea-level annual maxima (S_n) and associated daily maximum river discharge (q_n) within a defined time period centered on the date of S_n (+/- Δ days). The second one ~~uses~~ pairs river discharge annual maxima (Q_n) and associated hourly maximum sea levels (s_n) within a defined three days window ~~(Couasnon et al., 2020; Moftakhari et al., 2017; Sadegh et al., 2018)~~ centered on the date of Q_n (+/- one day) (Couasnon et al., 2020; Moftakhari et al., 2017; Sadegh et al., 2018). Each of the four sea level time-series observed and modelled records were then correlated with each of the three river discharge ones, which makes up a total of twelve different datasets (table A2).

2.2 Statistical analysis

- *Univariate analysis*

To estimate the extreme values of Nissan's river runoff and Halmstad sea levels, and their associated RPs, a GEV distribution was fitted to the annual extremes separately for each time series record (Coles, 2001; Ahsanullah, 2016). This was done using the MATLAB-based GEV-fitting algorithm, which provides parameter estimates and 95% confidence bands. Here, we do not make any assumption concerning the dependence between the two variables of interest, sea level and river discharge; each variable is modelled independently based on its own marginal distribution.

- *Bivariate analysis*

Initially, the Pearson, Spearman and Kendall's correlation coefficients and the associated p-values were calculated for each of the twelve collated data sets to assess whether there was a relationship between river runoff and sea level. The usual threshold value of 5% was defined as evidence for rejecting the H0 null hypothesis, that is, the two variables are independent. When p-values were found to be lower than the threshold, the null hypothesis could be rejected, and the two variables similarly found to show significant dependency. However, when p-values are above 5%, H0 cannot be rejected, so the two variables can be independent.

To represent the compound extremes, we apply copula modelling, which has been found to be useful for representing a joint probability (Hao et al., 2016). The analyses were carried out using the Multihazard Scenario Analysis Toolbox (MhAST), Version 2.0 from Sadegh et al., (2018). The ~~statistical~~ copula method models the dependence structure of the two random variables (Joe, 2014; Sadegh et al., 2017). It links or joins individual univariate distributions into a joint multivariate

distribution that has a specified correlation structure (Tootoonchi et al., 2022). The MhAST toolbox fits 25 different copulas to an input dataset. It first calculates the best possible fitting marginal distribution for each univariate dataset. It then proposes the best copula fit based on the Maximum Likelihood, Akaike Information Criterion (AIC), and the Bayesian Information Criterion (BIC). The root mean square error (RMSE) and Nash-Sutcliffe efficiency (NSE) values are calculated for each copula. Here, we evaluated the difference between each of the copula fits. An uncertainty analysis was also carried out using the MhAST toolbox with a "Weighted Average" and a "Maximum Density" approach (Sadegh et al., 2018). This first approach reproduces a distribution of potentially compound hazards. Based on the determined copula probability function, random samples are weighted accordingly and then calculated from the critical joint RP. The weights are determined based on the critical joint RP. This approach effectively generates a distribution of potential compound hazards while considering the underlying copula structure. This provides a comprehensive overview of the overall range of possible compound hazards. The second approach is based on the "most likely scenario" and provides an uncertainty range around it by adjusting the parameters of the copula distribution fit. Indeed, it focuses on first identifying the most likely scenarios for the compound hazard event which corresponds to the scenario with the highest density along the closed-form joint probability density function of the copula. This scenario is based on the copula fit parameters, which represent the statistical relationships between the individual hazard components. By adjusting these parameters, a range of possible most likely scenarios can be generated, allowing for the quantification of uncertainties around this central scenario.

Two types of Hazard Scenarios (HSs) have commonly been proposed to study the risk of compound floods related to sea level and river discharge (Salvadori et al., 2016; Moftakhari et al., 2019; Serinaldi, 2015). The "AND scenario" corresponds to a scenario where both the river discharge and the sea level are large enough to make a bivariate occurrence hazardous. The "OR scenario" corresponds to a scenario where either the river discharge or the sea level or both are large enough to make a bivariate occurrence troublesome.

2.3 Methodology

Firstly, a correlation analysis was carried out for each set, as proposed in section 2.2. This analysis investigated the significance of independence between the sea level and river discharge during extreme occurrences. Then, each set was used as input to the MhAST toolbox, which performed the compound analysis and returned 25 copula fits ranked depending on different criteria (section 2.2). Among the 25 copulas fitted, only the ones presenting a closed-form joint probability density function (Sadegh et al., 2017) were further investigated since, in these cases, "most likely scenarios" and their associated uncertainties can be defined. Chosen RLs were calculated for each copula, and their uncertainties were assessed. Adopting the "AND scenario" (see above) permitted us to investigate the risk of compound events only highlighting the dependency between sea level and river discharge during extreme events. Conversely, the "OR scenario" was finally preferred when looking at RLs as this looks into the "total" risk of flooding, whether originating from hydrological, coastal sources or both in combination.

To compare and evaluate the role of copulas and the role played by sea level and river discharge, respectively, a notion of normalized difference value (NDV) was introduced. We defined it as the normalized difference between the RL

values of interest from the bivariate analyses. Here, we normalize relative to the corresponding E-Hype univariate RL, which yields a representative dimensionless quantity. It should be pointed out that this quantity does not represent the "amplification" with respect to the univariate case since, as shown by Serinaldi (2015), one cannot compare RLs of different dimensionality. Suppose we investigate the resulting spread from using different copulas (based on the most likely scenarios within one set under the 5-year RP); the NDV is calculated as the difference between the maximum and minimum value of the most likely scenarios for any copula within a specific set divided by univariate 5-years RL derived from the E-Hype data set (section 3.2). When we look into the sensitivity of river discharge datasets, the sea level dataset is fixed, and the NDV is measured as the normalized difference between the maximum and minimum values of the most likely scenarios of best fits among the three sets of associated river discharge divided by the corresponding E-Hype univariate RL; and vice-versa, when looking into the sensitivity of sea level datasets. The NDV term indicates the magnitude of change or difference in RL results we can expect when choosing a certain copula or input dataset. Very small NDVs suggest that the corresponding choice of a variable of interest does not strongly influence the results. In contrast, large NDVs indicate that a particular choice results in significant differences.

3 Results and discussion

From the rank correlation analysis, the datasets based on sea level annual maxima (S_n, q_n) did not reveal any significant dependency (i.e., "compoundness") between sea level and river discharge, and therefore, no copula analysis was done (table A.1). In this case, the univariate analysis seemed to fit best under the proposed conditions of this study. Conversely, the datasets based on river discharge annual maxima (Q_n, s_n) yielded significant dependencies, suggesting a possible compound impact on river discharge. In the following subsections 3.1 and 3.3.1 we look into the "AND scenario" as we investigate the compound risk only. In the subsections 3.2 and 3.3.2, we mainly focus on the "OR scenario" (see above) as we are interested in the compound flood risk driven regardless of the situation (oceanographic or hydrological).

3.1 Dependency / Independency of the variables

Figure 5 and Table A1 show the dependency between the river discharge annual maxima and associated sea level local maxima (Q_n, s_n) event sets as expressed in section 2.1. Figure 5 displays the best copula distribution fit: BB1 from the rec Halmstad / E-Hype set under the "AND scenario" hypothesis for the 2, 5, 15 and 30-year RP. The full lines depict the RLs considering sea level and river discharge as dependent variables (derived from the best copula distribution fit). In contrast, the dashed lines show analogous results when assuming the two variables to be independent. The figure shows that the lines are not superposeddo not overlap, highlighting a dependency between both variables. Also, for all RLs presented, each RL from the independent hypothesis (dashed line) is placed below each corresponding RL from the dependent hypothesis (full line), supporting the hypothesis that compound events lead to higher flood risks when considering compound extremes as also found in Bevacqua et al. (2017) where they studied compound hydrological and oceanographic floods in Ravenna (Italy). Therefore,

 for example, a 30-year RP, when looking at the independent variables, would become a 13-year RP when considering the variables' dependency. This frequency increase comes from the compound effects and can be highlighted for each RP and copulas tested. Also, the dependency between extreme hydrological conditions and high oceanographic ones stresses the presence of compound effects, which lead to higher levels of river discharge and sea level during such events at the estuary. A copula-based joint probability density function is ~~assigned~~derived ~~to each copula fit curve~~, which permits obtaining a

295 probability of co-occurrences for a possible event along each curve, which is later used to carry out the uncertainty analysis (Sadegh et al., 2018). For example, along the 5-year RP curve, the probability of getting a 5-year RL of 180 $\underline{m^3\,s^{-1}}$~~m³/s~~ river discharge and 93 cm sea level is higher than getting one of 201 $\underline{m^3\,s^{-1}}$~~m³/s~~ and 20 cm or one of 101 $\underline{m^3\,s^{-1}}$~~m³/s~~ and a 112 cm one (fig. A1).

300
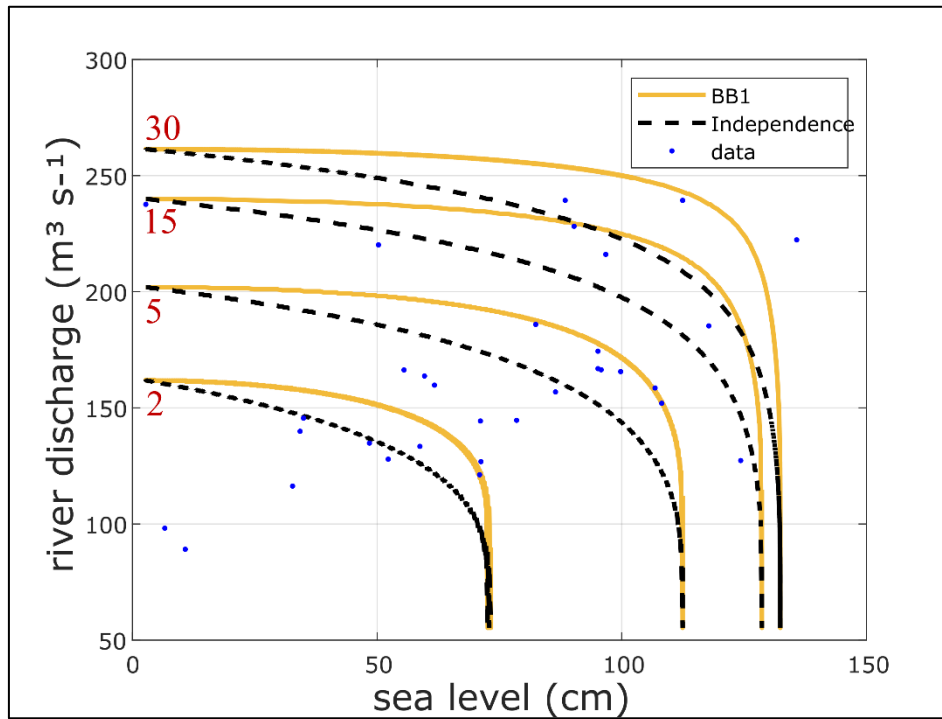
Figure 5: RLs for base case set rec Halmstad / E-Hype. Full lines correspond to the return period (RP) isolines for joint probability (AND scenario) of river discharge (y-axis) annual maxima and associated sea level (x-axis) maxima (Q_n, s_n). The dashed lines

305 **represent the distribution fit, assuming the independence between both variables. Blue dots show observed data. BB1 copula is used to model the dependence of river discharge annual maxima and associated sea level maxima calculated for each RPs visible in red text (2, 5, 15 and 30 years).**

3.2 Compound hazard potential on river floods

310   The focus is on river discharge RLs as a proxy for fluvial flooding indicators. Figure 6 represents the 5- and 30-year river discharge RLs from the set rec Halmstad / E-Hype under the "OR scenario" hypothesis for each copula tested and its associated uncertainties values from two approaches. The best copula fit selected based on the different criteria as AIC in this case (section 2.2) is BB1 (red diamond). The stars and diamonds represent the maximum density of the calculated RL for each copula, which can be interpreted as the most likely scenario under the bivariate analysis.

315

-      *RP = 5 years*

The 5-year RL from the E-Hype model is 201 $m^3\,s^{-1}$~~m³/s~~ with a 95th percentile confidence interval of 167-246 $m^3\,s^{-1}$~~m³/s~~ under the univariate GEV distribution fit. The BB1 copula fit has a 5-year RL "most likely scenario" of 220 $m^3\,s^{-1}$~~m³/s~~. Among all tested copulas, ~~The copulas'~~their 5-year RLs of "most likely scenarios" differ around 26 $m^3\,s^{-1}$~~m³/s~~, all between 208 and 234

320 $m^3\,s^{-1}$~~m³/s~~. The RL copulas' uncertainties are displayed with the boxplots from two methods: the "Weighted Average" approach showed with the outlined error bars, and the "Maximum Density" approach showed with the filled error bars. The "Weighted Average" approach gives more considerate uncertainty ranges than the "Maximum Density" (section 2.2). Indeed, for the best copula fit, the "Maximum Density" approach looking at the uncertainty of the "most likely scenarios" results in a narrow band of a maximum of 19 $m^3\,s^{-1}$~~m³/s~~ per copula against a more extensive range of 159 $m^3\,s^{-1}$~~m³/s~~ going from 202 to 361 $m^3\,s^{-1}$~~m³/s~~

325 with the "Weighted Average" approach. All copulas present a similar pattern.

Moreover, the RL uncertainties for the "Maximum Density" approach are all located within the 95th confidence interval of the univariate RL. However, the "Weighted Average" approach gives a 75th percentile of around 255 to 269 $m^3\,s^{-1}$~~m³/s~~ and a nonoutlier maximum of around 324 to 361 $m^3\,s^{-1}$~~m³/s~~ above the 246 $m^3\,s^{-1}$~~m³/s~~ corresponding to the 95th percentile of the univariate GEV fit, indicating the importance of considering bivariate analysis method. The BB1 copula chosen as the best fit

330 here by the different evaluation criteria mentioned in section 2.2 presents neither the smallest nor largest uncertainty band.

-      *RP = 30 years*

The 30-year RL from the E-Hype model is 263 $m^3\,s^{-1}$~~m³/s~~ with a 95th percentile confidence interval going from 189 to 431 $m^3\,s^{-1}$~~m³/s~~ under the univariate GEV distribution fit. The BB1 copula fit has a 30-year RL of 278 $m^3\,s^{-1}$~~m³/s~~. The copulas' 30-year

335 RL of "most likely scenarios" differ by around 25 $m^3\,s^{-1}$~~m³/s~~, with all of them between 267 and 292 $m^3\,s^{-1}$~~m³/s~~, except for the Gaussian copula. For all copulas except the Gaussian one, the "Weighted Average" approach gives a more extensive uncertainty range than the "Maximum Density" one. Indeed, for the best copula fit, the "Maximum Density" approach results in a relatively narrow band of 24 $m^3\,s^{-1}$~~m³/s~~, going from 272 to 296 $m^3\,s^{-1}$~~m³/s~~, against a more extensive range of 92 $m^3\,s^{-1}$~~m³/s~~ going from 261 to 353 $m^3\,s^{-1}$~~m³/s~~ with the "Weighted Average" one. All copulas except the Gaussian and the Tawn ones

340 present a similar pattern. Moreover, all RL uncertainties for both uncertainty analysis approaches are within the 95th confidence interval of the univariate RL for the 30-year RP.

- *Sensitivity to the choice of copula*

For both 5- and 30-year RPs, the copulas and their associated uncertainties present a similar pattern ~~with higher RLs when~~
~~considering the compound effects~~. Depending on the choice of copulas, the most likely scenarios differ up to 26 $\underline{m^3\,s^{-1}}$~~m³/s~~ for
the 5-year RP and up to 25 $\underline{m^3\,s^{-1}}$~~m³/s~~ for the 30-year RP, with the Tawn copula giving the minimum value and the Fischer-
Kock and FGM copulas giving the maximum value. When only looking at the most likely scenarios values for each copula,
they differ in a range approximately equal to 13% and 9.5% for the 5- and 30-year RPs, respectively (table A3). For each
copula, the uncertainties' relative errors based on the "Maximum Density" approach differ from 1% (Gaussian) to 9.9%
(Fischer-Kock) and from 2.3% (Joe) to 52% (Gaussian) for the 5- and 30-year RPs respectively; from 63% (Joe) to 75%
(Fischer-Kock) and from 16% (Joe) to 35% (Fischer-Kock) for the "Weighted Average" approach. For comparison, the relative
errors for the univariate GEV fit are around 41% and 92% for the 5- and 30-year RPs, respectively. When considering the
"Maximum Density" uncertainties, all RLs of all copula are in the range of 208-234 $\underline{m^3\,s^{-1}}$~~m³/s~~ for the 5-year RL and 262-398
$\underline{m^3\,s^{-1}}$~~m³/s~~ for the 30-year RL (Table A3; fig. 6).

These differences in resulting RLs emphasize the importance of the role played by the choice of copulas and the consideration
of quantifying uncertainties.
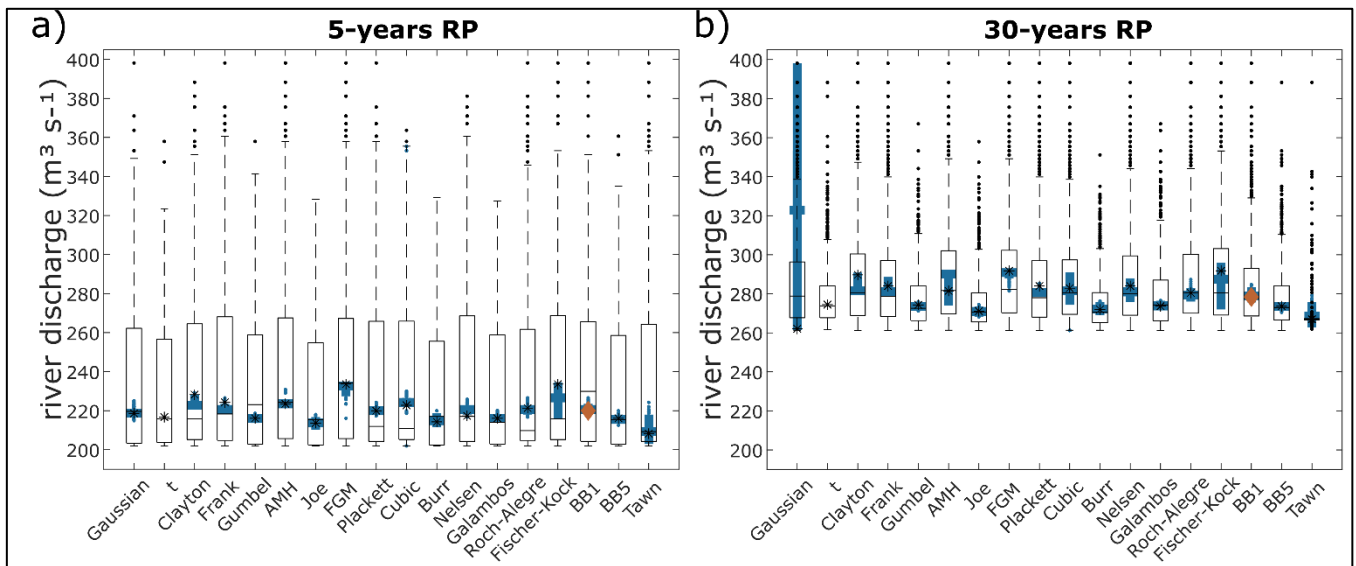
**Figure 6: Fluvial component in bivariate events with 5- (a) and 30-year (b) ~~RLs~~ Return periods ~~of river discharge~~ from copula fits
~~and univariate GEV fits~~ for rec Halmstad / E-Hype. Each column represents a copula distribution fit. Stars represent the most likely
scenario return values from each copula for each set, and the red diamond is the best copula fit. Two uncertainty approaches are
displayed as boxplots, giving a statistical summary. Median, first, and third quartiles are represented in each box, whiskers represent
minimum/maximum values, and dots represent outliers. Outlined boxplots correspond to the "Weighted Average" approach, and
filled ones to the "Maximum Density" approach.**

3.3 Sensitivity analysis on compound flood hazard potential -OR scenario-

This section focuses on the impact of data sources on resulting RP statistics, aiming to compare copula analyses considering compound events. As seen in section 2.1, we have twelve possible data sets to analyze for Halmstad city extracted from models and observations. As mentioned in section 2.1, the univariate analysis presents different results, including RL
370 values and confidence intervals for each river runoff time series.

5-year and 30-year univariate RLs of river runoff, respectively, differ by around 9 $m^3 s^{-1}$ ~~m³/s~~ and 21 $m^3 s^{-1}$ ~~m³/s~~ with values of 202 $m^3 s^{-1}$ ~~m³/s~~ and 241 $m^3 s^{-1}$ ~~m³/s~~ based on observation gauge (red); 193 $m^3 s^{-1}$ ~~m³/s~~ and 252 $m^3 s^{-1}$ ~~m³/s~~ based on S-Hype model (blue); 201 $m^3 s^{-1}$ ~~m³/s~~ and 263 $m^3 s^{-1}$ ~~m³/s~~ based on E-Hype model (green) as displayed in Figure 4-b. However, uncertainties associated with the 95th percentile confidence interval differ vastly from respectively around 86 $m^3 s^{-1}$ ~~m³/s~~ and 185 $m^3 s^{-1}$ ~~m³/s~~
375 (observation); 121 $m^3 s^{-1}$ ~~m³/s~~ and 811 $m^3 s^{-1}$ ~~m³/s~~ (S-Hype); 79 $m^3 s^{-1}$ ~~m³/s~~ and 242 $m^3 s^{-1}$ ~~m³/s~~ (E-Hype) as displayed with the background colours on the figure.

3.3.1 Dependency / Independency of the variables

Figure 7 presents resulting RLs for combined ranges of each variable set for the 5- and 30-year RPs as in Figure 5, but with results from six different data sources to study the resulting impacts. The dependency is evident for each set, with
380 each full line moved away from its corresponding dashed line, highlighting the dependency and compound effects for any sets tested. The differences between solid and dashed lines in Figure 7 are typically contained within about 20 cm sea level or 25 $m^3 s^{-1}$ ~~m³/s~~ river discharge, constituting about 10-15% of the extreme 5- and 30-year RLs for the site with a gap increasing with higher RPs. At first glance, these differences may be perceived as a reasonably small compound effect, but every little increase in extreme situations can have a consequence for society. It should be noted that switching data sources may have a ~~more~~
385 significant effect on estimated RLs; hence, both method and choice of data are essential.
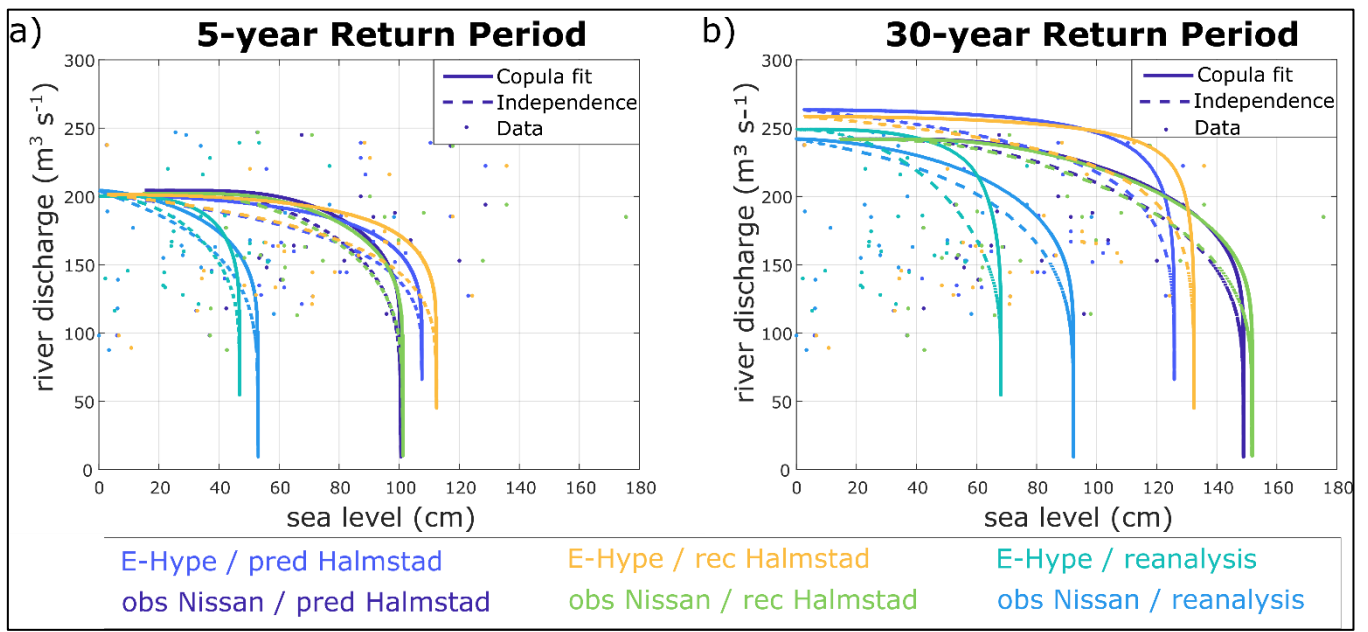
Figure 7: 5- (a) and 30-year (b) Return periods isolines for joint probability (AND scenario) of river discharge (y-axis) annual maxima and associated sea level (x-axis) maxima (Q_n, s_n) for Halmstad. Full lines implement the compound effect, and dashed lines represent fit, assuming independence between both variables. Dots show observed data. The best copula fit is used to model the dependence of (Q_n, s_n) calculated for each set visible in coloured text.

Some sets behave similarly as their corresponding dashed and full lines ~~are~~ almost ~~superposed~~ overlap as for the sets obs Nissan / pred Halmstad & obs Nissan / rec Halmstad or E-Hype / pred Halmstad & E-Hype / rec Halmstad in both 5- and 30-year RPs (fig. 7). This similarity ~~stresses the idea~~emphasizes that river discharge ~~pre~~dominates over sea-level inputs the co-occurrence probabilities of bivariate hazardous events.

3.3.2 Compound hazard potential on river floods

The most likely scenarios of 5- and 30-year RPs and their associated uncertainties on the different sets are calculated as described in section 2.1. This study focuses on extreme hydrological events associated with oceanographic conditions and, therefore, concentrates on the RLs of river discharge. Figure A2 displays those results for each set in the same way as Figure 6. Figure A2-a returns the results of the 5-year RP and Figure A2-b, the 30-year RP analysis.

Under the 5-year RP, lower RLs are found for all obs sea level sets (fig. A2-a), corresponding to the data available and short duration of overlapping periods, with a maximum of 13 years and limited by the extent of sea level observations. Under the 30-year RP, lower RLs are found for the set E-Hype / obs sea level and all S-Hype sets except for S-Hype / obs sea level, which presents the most extreme values.

For the 5- and 30-year RPs, the three sets associated with the E-Hype model, which show statistical significance, lead to similar and higher values, respectively, than all the other sets. The last set showing statistical significance is associated with

the S-Hype model and leads to somewhat different results between the 5-year RP, with slightly lower RLs, and the 30-year RP, with generally higher RLs (fig. A2). It stresses that the dependence changes the RP results as also shown by Santos et al. (2021) which studied compound surge and precipitation events in a case study in the Netherlands.

All most likely scenario values calculated from the copula analysis under both the 5- and 30-year RPs are within the range of the 95th percentile confidence interval of the univariate GEV distribution fit (fig. A2). Uncertainties associated with the copula analysis and following the "Maximum Density" approach do not extend too much from the median values and stay within the confidence interval of the univariate GEV distribution (fig. A2) for most of the copulas tested. Under this "Maximum Density" approach and based on the best copula fits, they differ by about 3-8 $m^3 s^{-1}$ ~~m³/s~~ for the 5-year RP and 2-9 $m^3 s^{-1}$ ~~m³/s~~ for the 30-year RP. Under those same conditions, the uncertainties from the "Weighted Average" approach vary between 65 and 149 $m^3 s^{-1}$ ~~m³/s~~ for the 5-year RP and between 37 and 68 $m^3 s^{-1}$ ~~m³/s~~ for the 30-year RP. Therefore, uncertainties related to the "Maximum Density" approach associated with the most likely scenarios are relatively small, providing reasonable confidence in such scenarios. Conversely, the "Weighted Average" approach uncertainties provide a confidence interval on possibly more extreme scenarios, which is relevant when communicating RLs.

- ***Input datasets selection***

Depending on the choice of river time series as initial input, the results of the copula analysis under the 5- and 30-year RPs differ substantially around a maximum of 20 $m^3 s^{-1}$ ~~m³/s~~ and 40 $m^3 s^{-1}$ ~~m³/s~~, respectively, with an NDV range of 6-10% and 8.4-15% (fig. 8). This contrasts with the choice of sea level time series as initial input with a maximum difference of around 6 and 12 $m^3 s^{-1}$ ~~m³/s~~ equivalent to 1.5-3% and 2.3-4.6% NDV bounds for the 5- and 30-year RPs, respectively, without considering the three sets associated with obs sea level. Those results are based on the most likely scenarios from each best copula fit and did not consider the obs sea level associated sets. It emphasizes that the choice of sea level records has a lower influence than the one of river discharge within this study on compound hydrological extreme events on our example study site (Halmstad). The well-recognized issues from the reanalysis dataset support this result as even a large difference in the sea level input dataset does not get reflected in the NDV values when looking at the choice of sea level. Similar ~~results~~ findings could be expected for the surrounding area (West coast of Sweden).

- ***Copula selection***

To evaluate the role played by choice of the copula, we calculated the NDV for each set between the maximum and the minimum values returned by the 18 copulas tested without considering the sets with obs sea level data input as it was too short for bivariate analysis. Among all the different sets, the BB1, the Gaussian and the Clayton copulas are the best ones based on the different statistical criteria (section 2.2). Moreover, when only looking at the sets associated with the same river runoff input, the best copula fit is the same: Clayton for obs Nissan, BB1 for E-Hype except for S-Hype, which has Gaussian as the best fit for S-Hype/rec Halmstad and Clayton for the two other sets. The tests of using multiple copulas have also been investigated in previous studies. Lucey and Gallien (2022) looked at compound coastal events linking precipitation and/or sea

level in a tidal and semi-arid area. They noticed that, in their particular area, the Nelsen, BB1, BB5, and Roch-Alegre copulas represented best their datasets and each of them provided similar results in almost all cases. Bai et al. (2020) introduced a mixed copula which is a linear combination of Gumbel, Clayton, and Frank copulas to statistically study coastal winds and

445   waves. They observed that the mixed copula can better describe the dependency structure than the five single copulas tested (Gaussian, t, Gumbel, Clayton, Frank) where the representation of relations between both drivers is complex.

For most of the sets, the "Fischer-Kock" and the "FGM" copulas give the highest RLs and the "Tawn" and "Joe" copulas give the smallest ones (fig. A2). It results in NDVs between 5.5% and 13% for the 5-year RP and between 3.8% and 9.5% for the 30-year RP. The base case E-Hype / rec Halmstad presents the highest NDVs when comparing with other sets NDVs, which

450   emphasizes that the choice of copula is relatively more important than in other sets (fig. 8). Based on our assumption that this is possibly the best set, in terms of data sources, it stresses the idea that the choice of copula becomes more and more critical when input datasets are long enough and statistically significant.

Therefore, the choice of copula has a similar influence as the choice of river discharge records for each of the nine sets tested here, as the obs sea level has not been considered. For both the 5- and 30-year RPs, the choice of sea level is the least impactful.

455   Under the 5-year RP, the choice of copula is overall the most important before the choice of river discharge, but under the 30-year RP, the choice of river discharge predominates. However, this differs when looking at specific sets' copula NDVs (fig. 8).
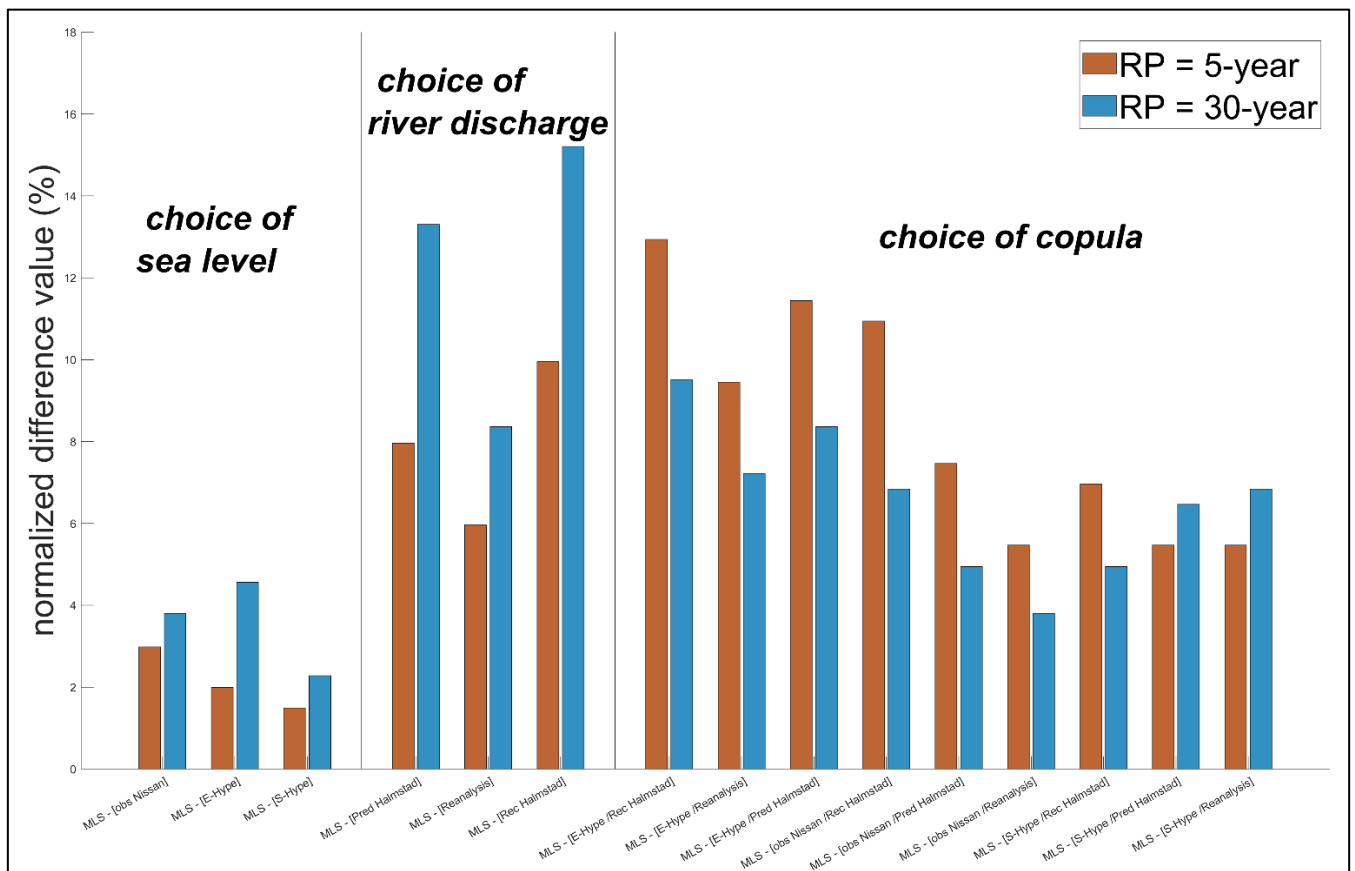
Figure 8: Normalized difference values (%) for evaluating the importance of copula fit and forcing data for both 5- and 30-year
rReturn pPeriods as mentioned in section 3.3.2.

4 Limitations

Observed time-series datasets have a relatively short length, leading to rather high uncertainties once applying the GEV analysis. Similarly, model time-series datasets have inherent uncertainties, which can be challenging to quantify. Various data sources were assessed for their applicability in bivariate analysis, and direct sea level observations available for only 13 years were a limiting factor. We focus on longer reconstructed time series and other data sources for the principal analysis. Moreover, assumed stationarity within the datasets can be a limitation while performing the statistical analysis (Kudryavtseva et al., 2021). The choice of the sampling datasets based on annual maxima can be a limitation. For instance, in their specific tidal dominated and semi-arid area, Lucey and Gallien (2022) stated that annual maximum sampling seems to underestimate water levels at longer RPs. In this study, only the compounding between sea level and river discharge has been studied but Latif and Simonovic (2023) showed that considering the three drivers storm surge, precipitation and river discharge to study compound coastal floods can provide a better statistical approach and therefore better estimate joint RPs in their study area

located on the West Coast Canada. However, after carrying out a brief sensitivity analysis on defining extreme sea level events as sea level peaks above the 95th or 99th percentile and comparing it with the annual maxima sampling, no noticeable changes were found; a similar conclusion was also drawn by Ward et al. (2018).

A compound analysis is seen as a relatively new approach within this field of study, which also involves some limitations, such as the quantification of uncertainties within a multivariate analysis that differ widely depending on the choice of a copula. The uncertainty resulting from the choice of copula can to some extent be constrained by adopting appropriate goodness-of-fit statistics for the selection of the best-fitting copula. In this study, we choose to illustrate this indirectly by presenting results from many different choices of copula, despite having calculated such goodness-of-fit metrics (section 2.2). Furthermore, we showed the normalized difference values for different data sources. As discussed in section 2.3 and Serinaldi (2015) a careful interpretation comparing return levels from different methodologies is, however, always needed. In decision-making adapting a strategy such as ours (to include results from all studied copulas and also different data sources) has some limitations in the sense that too much information can sometimes cause more confusion than help for the decision. Often it may be possible to argue against some choices of copulas (e.g. the Gaussian copula when the distributions are skewed) and the strategy of constraining the results to one copula or a set of "best-fitting" copulas using some threshold on the goodness-of-fit metrics may be appropriate. For the purpose of our study and the conclusion drawn we consider, however, that presenting the results from multiple choices of data and multiple copula is appropriate.

5 Summary and conclusions

This study assesses the hydrological and oceanographic processes that may lead to compound flood effects in Halmstad. The method is easily transferable to other regions or sites. In the paper, we stress the importance of the choice of data sources and copulas for multivariate analysis. Based on our analysis, we conclude that:

• A dependency is found between the annual maxima of river discharge and the corresponding sea level. The ~~opposite~~ dependency for annual sea level maxima and associated river discharge was not considered significant at this site.

• All values of the "most likely" scenarios and their uncertainties resulting from the copula analysis are within the range of the 95th percentile confidence interval of the univariate GEV distribution fit.

• The choice of river time series as initial input influences the results of the copula analysis to a higher degree than the choice of sea level time series as initial input.

• ~~The choice of copula has a similar magnitude of its influence on return period statistics as the choice of river discharge input~~ Copula choice has a similar influence on return period statistics as the river discharge input for most of the twelve sets tried.

• According to statistical criteria, the Clayton, BB1 and Gaussian (once) copulas performed the best in this study.

505 Uncertainties in compound flood hazard quantification are essential to consider. They can come from different sources, such as methodology and data sources. This study stresses the importance of the choice of data sources and copula.

5 Appendices

Table A1: Rank correlation (rho) and p-values of the twelve different sets based on (Q_n/ s_n) in columns: " / river" and (q_n/ S_n) in columns " / sea" ; the best set of study is displayed with bold and underlined; p_values above 5% are highlighted in italic.

river	sea level	rank correlation	rho / river	p / river	rho / sea	p / sea
E-Hype	reanalysis	Pearson	0.4532	0.0154	*0.0443*	*0.8227*
		Kendall	0.3280	0.0141	*0.0370*	*0.7992*
		Spearman	0.4532	0.0163	*0.0443*	*0.8226*
obs Nissan		Pearson	*0.2430*	*0.2478*	0.6684	*0.0922*
		Kendall	*0.2896*	*0.1594*	0.6410	*0.0725*
		Spearman	*0.2419*	*0.2478*	0.6674	*0.0922*
S-Hype		Pearson	*0.3799*	*0.1325*	-0.0760	*0.7719*
		Kendall	*0.3088*	*0.0914*	-0.0588	*0.7765*
		Spearman	*0.3799*	*0.1333*	-0.0760	*0.7729*
E-Hype	observed	Pearson	*0.4725*	*0.1030*	*0.4056*	*0.1908*
		Kendall	*0.3590*	*0.1000*	*0.2424*	*0.3108*
		Spearman	*0.4725*	*0.1057*	*0.4056*	*0.1926*
obs Nissan		Pearson	*0.4396*	*0.1329*	-0.1049	*0.7456*
		Kendall	*0.3333*	*0.1289*	-0.0606	*0.8406*
		Spearman	*0.4396*	*0.1350*	-0.1049	*0.7495*
S-Hype		Pearson	0.6273	0.0388	-0.0490	*0.8799*
		Kendall	0.4909	0.0405	-0.0303	*0.9466*
		Spearman	0.6273	0.0440	-0.0490	*0.8863*
E-Hype	pred Viken	Pearson	0.4439	0.0109	*0.2438*	*0.1788*
		Kendall	0.3145	0.0111	*0.1452*	*0.2518*
		Spearman	0.4439	0.0116	*0.2438*	*0.1782*
obs Nissan		Pearson	*0.3400*	*0.1040*	*0.2435*	*0.2516*
		Kendall	*0.2319*	*0.1189*	*0.1522*	*0.3128*
		Spearman	*0.3400*	*0.1044*	*0.2435*	*0.2505*
S-Hype		Pearson	*0.3676*	*0.1466*	*0.2843*	*0.2687*
		Kendall	*0.2794*	*0.1288*	*0.1912*	*0.3081*
		Spearman	*0.3676*	*0.1471*	*0.2843*	*0.2678*
E-Hype	***rec Viken***	Pearson	**0.4836**	**0.0044**	*0.2753*	*0.1273*

		Kendall	**0.3523**	**0.0036**	**0.1815**	**0.1500**
		Spearman	**0.4836**	**0.0048**	**0.2753**	**0.1272**
obs Nissan		Pearson	*0.3446*	*0.0916*	*0.1487*	*0.4880*
		Kendall	*0.2333*	*0.1076*	*0.1014*	*0.5071*
		Spearman	*0.3446*	*0.0921*	*0.1487*	*0.4863*
S-Hype		Pearson	*0.4882*	*0.0550*	*0.1373*	*0.5994*
		Kendall	0.3833	0.0413	*0.1029*	*0.5976*
		Spearman	*0.4882*	*0.0572*	*0.1373*	*0.5986*

510

Table A2: Summary report of runs from ~~MhAST~~ the copula analysis for the twelve different sets; the best study set is highlighted in bold, italic and underlined.

river	sea level	Copula best fit	number of co-occurring years
obs Nissan	reanalysis	Clayton	24
	obs sea level	Galambos	13
	pred Halmstad	Clayton	24
	rec Halmstad	Clayton	25
E-Hype	reanalysis	BB1	28
	obs sea level	Gaussian	13
	pred Halmstad	BB1	32
	rec Halmstad	*BB1*	*33*
S-Hype	reanalysis	Clayton	17
	obs sea level	BB1	11
	pred Halmstad	Clayton	17
	rec Halmstad	Gaussian	16

Table A3: Summary report from the river discharge's results and associated uncertainties from ~~MhAST~~ the copula analysis for
515 **the E-Hype / rec Halmstad set; the results from the univariate method are highlighted in bold, italic and underlined. The Gaussian copula has not been considered for the analysis of the "most likely scenarios" row.**

E-Hype / rec Halmstad	copula distribution fit		5-years RL	30-years RL
univariate		*median*	*201*	*263*
		max 95%	*250*	*431*
		min 5%	*167*	*189*
		relative error	*41.29%*	*92.02%*

"most likely scenarios"	Fischer-Kock / FGM	max copula	234	292
	Tawn	min copula	208	267
	NDV		*12,94%*	*9,51%*
uncertainties "Maximum Density" approach	BB1	max without ouliers	224	284
	BB1	min without ouliers	218	276
	BB1	*NDV*	*2,99%*	*3,04%*
	Joe	max without ouliers	217	274
	Joe	min without ouliers	210	268
	Joe	*NDV*	*3,48%*	*2,28%*
	Fischer-Kosck	max without ouliers	235	296
	Fischer-Kosck	min without ouliers	215	272
	Fischer-Kosck	*NDV*	*9,95%*	*9,13%*
	Gaussian	max without ouliers	220	398
	Gaussian	min without ouliers	218	262
	Gaussian	*NDV*	*1,00%*	*51,71%*
uncertainties "Weighted Average" approach	BB1	max without ouliers	351	329
	BB1	min without ouliers	202	261
	BB1	*NDV*	*74,13%*	*25,86%*
	Joe	max without ouliers	328	303
	Joe	min without ouliers	202	261
	Joe	*NDV*	*62,69%*	*15,97%*
	Fischer-Kosck	max without ouliers	353	353
	Fischer-Kosck	min without ouliers	202	261
	Fischer-Kosck	*NDV*	*75,12%*	*34,98%*
	Gaussian	max without ouliers	349	338
	Gaussian	min without ouliers	202	261

	Gaussian	*NDV*	*73.13%*	*29.28%*
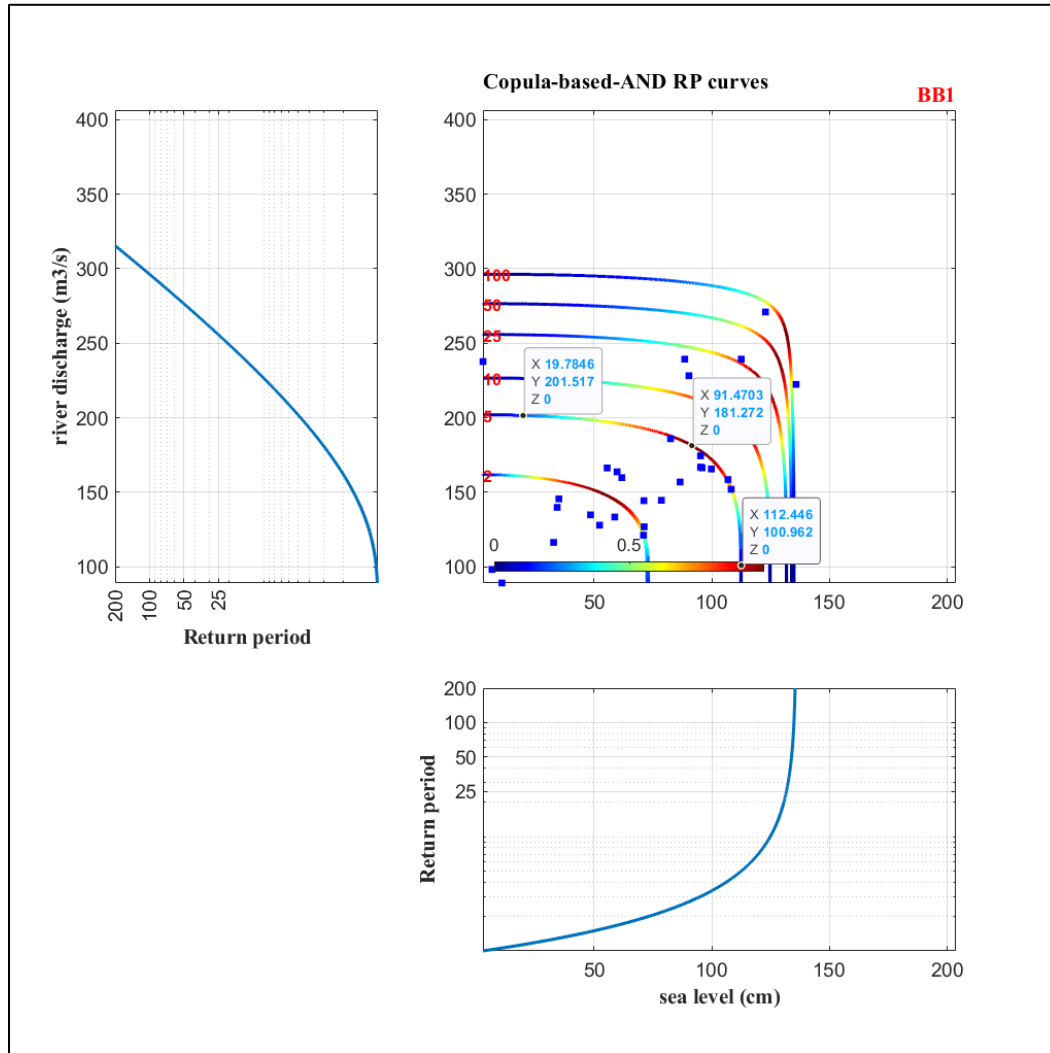
Figure A1: Set E-Hype / rec Halmstad, best copula fit: BB1. [2, 5, 10, 25, 50, 100] RPs and associated densities. The left and lower panels correspond to marginal RPs curves of each univariate parameter individually, river discharge and sea level (extracted from MhAST software).

520
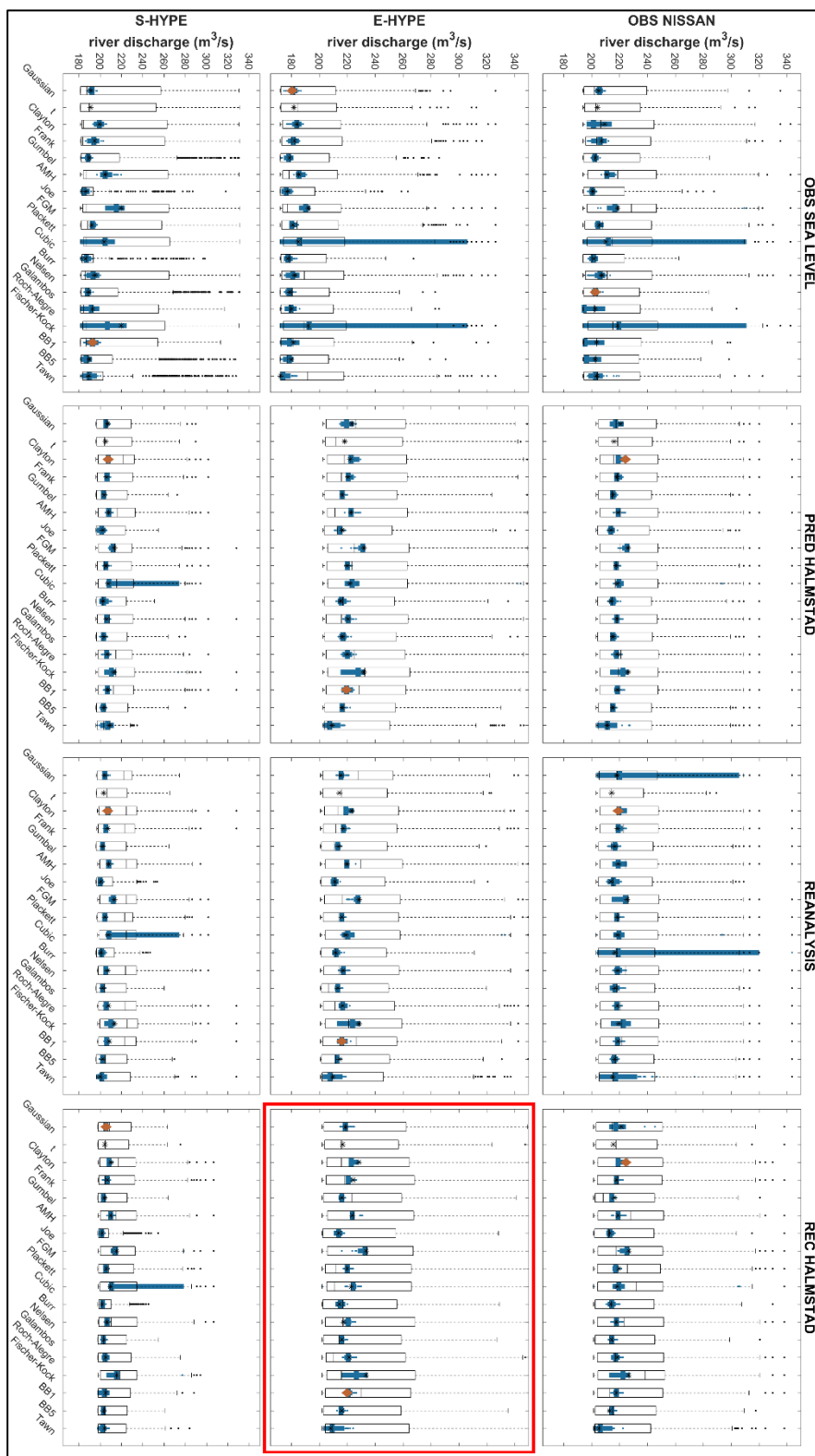
Fig. A2-a)

Fig. A2-b)
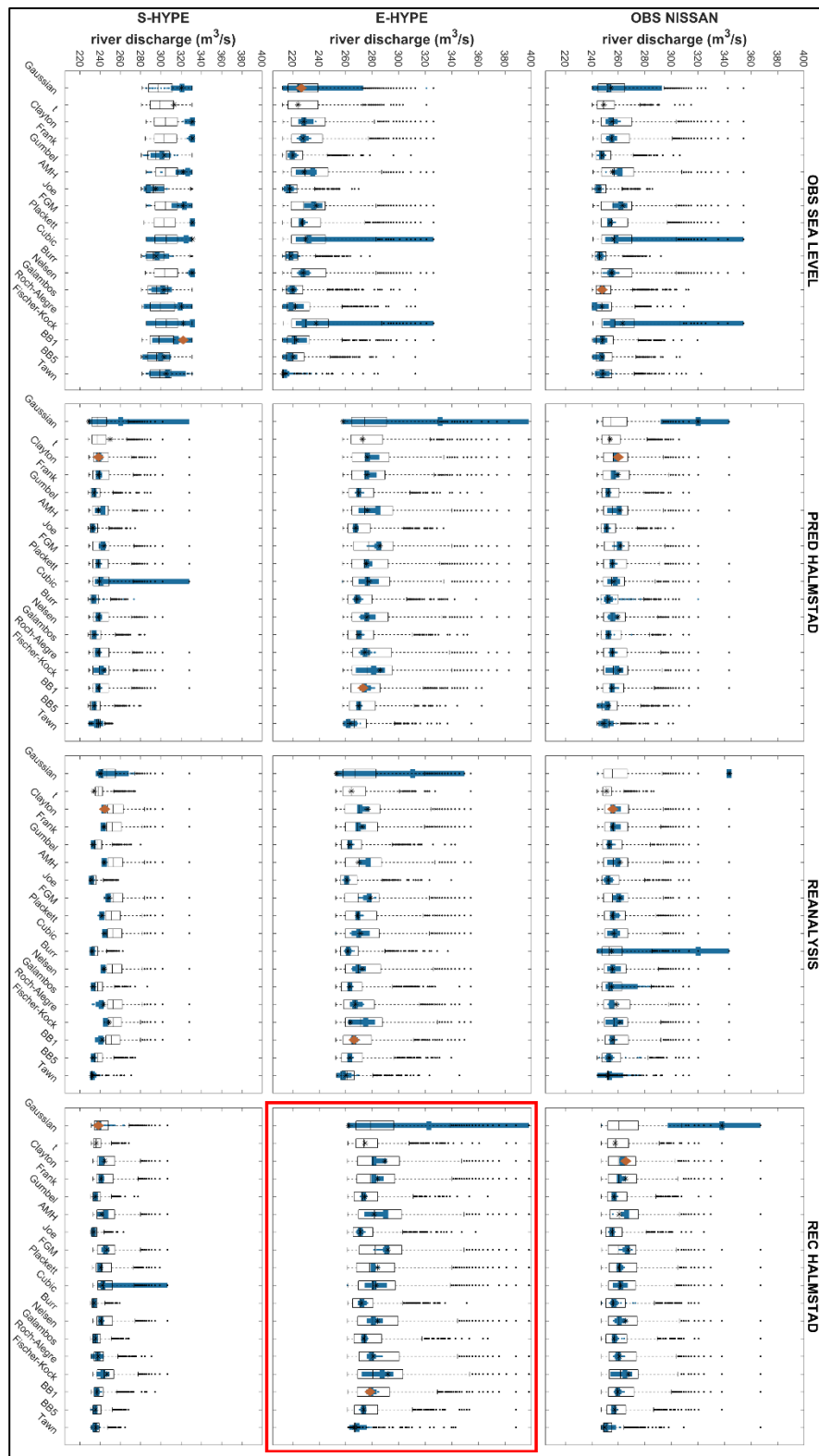
Figure A2: Fluvial component in bivariate events with 5- (a) and 30-year (b) RPs values ~~of river discharge~~ from copula fits ~~and univariate GEV fits~~. **Each subplot corresponds to a set of events from an association of river discharge and sea level inputs displayed as a matrix, and in each column, a copula distribution fit where two uncertainty approaches are displayed as error bars. Stars represent the most likely scenarios return values from each copula for each set and each red diamond, the best-fit copula. The two uncertainty approaches are displayed as boxplots that give a statistical summary. Median, First and third quartiles are represented in each box; Whiskers represent minimum and maximum values, and dots represent outliers. Outlined boxplots correspond to the "Weighted Average" approach, and filled ones to the "Maximum Density" approach. The set E-Hype / Rec Halmstad, used as a base case, is highlighted by the red rectangles.**

Code availability. The code used to generate the figures can be acquired by contacting the first author (kevin.dubois@geo.uu.se).

Data availability. Observations data are available from SMHI at https://www.smhi.se/data/oceanografi/ladda-ner-oceanografiska-observationer#param=sealevelrh2000,stations=core for the sea level (accessed on: 14th of October 2021) and https://vattenweb.smhi.se/station/ for the river discharge (accessed on: 28th of April 2021).

Author contributions. KD conducted the analysis. KD prepared the manuscript with contributions from all co-authors.

Competing interests. The authors declare that they have no conflict of interests.

Acknowledgements. The work forms part of the project: Extreme events in the coastal zone – a multidisciplinary approach for better preparedness. The authors would like to thank the three anonymous reviewers for their valuable comments which contributed to improving the quality of the paper. We further thank Johanna Mård, Christoffer Hallgren and Faranak Tootoonchi for our useful discussions.

Financial support. This research was funded by the Swedish Research Council FORMAS (Grant No. 2018-01784) and the Centre of Natural Hazards and Disaster Science (CNDS).

References

Aghakouchak, A., Chiang, F., Huning, L. S., Love, C. A., Mallakpour, I., Mazdiyasni, O., Moftakhari, H., Papalexiou, S. M., Ragno, E., and Sadegh, M.: Climate Extremes and Compound Hazards in a Warming World, Annu. Rev. Earth Planet. Sci., 48, 519–548, https://doi.org/10.1146/annurev-earth-071719-055228, 2020.

Ahsanullah, M.: Extreme value distributions, edited by: Chris P. Tsokos, Tampa, U., https://doi.org/10.2991/978-94-6239-222-9 137, 2016.

Andrée, E., Su, J., Andreas Dahl Larsen, M., Drews, M., Stendel, M., and Madsen, K. S.: The role of preconditioning for extreme storm surges in the western Baltic Sea, Nat. Hazards Earth Syst. Sci., 23, 1817–1834, https://doi.org/https://doi.org/10.5194/nhess-23-1817-2023, 2023.

Bai, X., Jiang, H., Li, C., and Huang, L.: Joint probability distribution of coastal winds and waves using a log-transformed kernel density estimation and mixed copula approach, Ocean Eng., 216, https://doi.org/10.1016/j.oceaneng.2020.107937, 2020.

Bergstrand, M., Asp, S. S., and Lindström, G.: Nationwide hydrological statistics for Sweden with high resolution using the hydrological model S-HYPE, Hydrol. Res., 45, 349–356, https://doi.org/10.2166/nh.2013.010, 2014.

Bevacqua, E., Maraun, D., Hobæk Haff, I., Widmann, M., and Vrac, M.: Multivariate statistical modelling of compound events via pair-copula constructions: Analysis of floods in Ravenna (Italy), Hydrol. Earth Syst. Sci., 21, 2701–2723, https://doi.org/10.5194/hess-21-2701-2017, 2017.

Bevacqua, E., Maraun, D., Vousdoukas, M. I., Voukouvalas, E., Vrac, M., Mentaschi, L., and Widmann, M.: Higher probability of compound flooding from precipitation and storm surge in Europe under anthropogenic climate change, Sci. Adv., 5, 1–8, https://doi.org/10.1126/sciadv.aaw5531, 2019.

CMEMS: For Baltic Sea Physical Reanalysis Products :, 1–27, https://doi.org/https://doi.org/10.48670/moi-00013, 2022.

Coles, S.: An Introduction to Statistical Modeling of Extreme Values, Technometrics, 44, 397–397, https://doi.org/10.1198/tech.2002.s73, 2001.

Couasnon, A., Eilander, D., Muis, S., Veldkamp, T. I. E., Haigh, I. D., Wahl, T., Winsemius, H. C., and Ward, P. J.: Measuring compound flood potential from river discharge and storm surge extremes at the global scale, Nat. Hazards Earth Syst. Sci., 20, 489–504, https://doi.org/10.5194/nhess-20-489-2020, 2020.

Crameri, F., Shephard, G. E., and Heron, P. J.: The misuse of colour in science communication, Nat. Commun., 11, 1–10, https://doi.org/10.1038/s41467-020-19160-7, 2020.

Dacre, H. F., Hawcroft, M. K., Stringer, M. A., and Hodges, K. I.: An extratropical cyclone atlas a tool for illustrating cyclone structure and evolution characteristics, Bull. Am. Meteorol. Soc., 93, 1497–1502, https://doi.org/10.1175/BAMS-D-11-00164.1, 2012.

Donnelly, C., Andersson, J. C. M., and Arheimer, B.: Using flow signatures and catchment similarities to evaluate the E-HYPE multi-basin model across Europe, Hydrol. Sci. J., 61, 255–273, https://doi.org/10.1080/02626667.2015.1027710, 2016.

Dubois, K., Larsen, M. A. D., Drews, M., Nilsson, E., and Rutgersson, A.: Technical note: Extending sea level time series for the analysis of extremes with statistical methods and neighbouring station data, Ocean Sci., 20, 21–30, https://doi.org/10.5194/os-20-21-2024, 2024. Dubois, K., Andreas Dahl Larsen, M., Drews, M., Nilsson, E., and Rutgersson, A.: Technical note : Extending sea level time series for extremes analysis with machine learning and neighbouring station data, Egusph. [preprint], 1–14, https://doi.org/https://doi.org/10.5194/egusphere-2023-1159, 2023, 2023.

Eilander, D., Couasnon, A., Ikeuchi, H., Muis, S., Yamazaki, D., Winsemius, H. C., and Ward, P. J.: The effect of surge on riverine flood hazard and impact in deltas globally, Environ. Res. Lett., 15, https://doi.org/10.1088/1748-9326/ab8ca6, 2020.

Feng, D., Tan, Z., Engwirda, D., Liao, C., Xu, D., Bisht, G., Zhou, T., Li, H. Y., and Leung, L. R.: Investigating coastal backwater effects and flooding in the coastal zone using a global river transport model on an unstructured mesh, Hydrol. Earth Syst. Sci., 26, 5473–5491, https://doi.org/10.5194/hess-26-5473-2022, 2022.

590 Ganguli, P. and Merz, B.: Extreme Coastal Water Levels Exacerbate Fluvial Flood Hazards in Northwestern Europe, Sci. Rep., 9, 1–14, https://doi.org/10.1038/s41598-019-49822-6, 2019.

Gori, A., Lin, N., and Xi, D.: Tropical Cyclone Compound Flood Hazard Assessment: From Investigating Drivers to Quantifying Extreme Water Levels, Earth's Futur., 8, https://doi.org/10.1029/2020EF001660, 2020.

Hao, Z. and Singh, V. P.: Review of dependence modeling in hydrology and water resources, Prog. Phys. Geogr., 40, 549–
595 578, https://doi.org/10.1177/0309133316632460, 2016.

Hendry, A., Haigh, I. D., Nicholls, R. J., Winter, H., Neal, R., Wahl, T., Joly-Lauge, A., and Darby, S. E.: Assessing the characteristics and drivers of compound flooding events around the UK coast, Hydrol. Earth Syst. Sci., 23, 3117–3139, https://doi.org/10.5194/hess-23-3117-2019, 2019.

Hieronymus, M. and Kalén, O.: Sea-level rise projections for Sweden based on the new IPCC special report: The ocean and
600 cryosphere in a changing climate, Ambio, 49, 1587–1600, https://doi.org/10.1007/s13280-019-01313-8, 2020.

Hieronymus, M. and Kalén, O.: Should Swedish sea level planners worry more about mean sea level rise or sea level extremes?, Ambio, 51, 2325–2332, https://doi.org/10.1007/s13280-022-01748-6, 2022.

Hieronymus, M., Hieronymus, J., and Hieronymus, F.: On the application of machine learning techniques to regression problems in sea level studies, J. Atmos. Ocean. Technol., 36, 1889–1902, https://doi.org/10.1175/JTECH-D-19-0033.1, 2019.

605 Hoskins, B. J. and Hodges, K. I.: New perspectives on the Northern Hemisphere winter storm tracks, J. Atmos. Sci., 59, 1041–1061, https://doi.org/10.1175/1520-0469(2002)059<1041:NPOTNH>2.0.CO;2, 2002.

Jane, R. A., Malagón-Santos, V., Rashid, M. M., Doebele, L., Wahl, T., Timmers, S. R., Serafin, K. A., Schmied, L., and Lindemer, C.: A Hybrid Framework for Rapidly Locating Transition Zones: A Comparison of Event- and Response-Based Return Water Levels in the Suwannee River FL, Water Resour. Res., 58, https://doi.org/10.1029/2022WR032481, 2022.

610 Joe, H.: Dependence modeling with copulas, Depend. Model. with Copulas, 1–457, https://doi.org/10.1201/b17116, 2014.

Kiesel, J., Lorenz, M., König, M., Gräwe, U., and Vafeidis, A. T.: Regional assessment of extreme sea levels and associated coastal flooding along the German Baltic Sea coast, Nat. Hazards Earth Syst. Sci., 23, 2961–2985, https://doi.org/10.5194/nhess-23-2961-2023, 2023.

Kudryavtseva, N., Soomere, T., and Männikus, R.: Non-stationary analysis of water level extremes in Latvian waters, Baltic
615 Sea, during 1961-2018, Nat. Hazards Earth Syst. Sci., 21, 1279–1296, https://doi.org/10.5194/nhess-21-1279-2021, 2021.

Latif, S. and Simonovic, S. P.: Compounding joint impact of rainfall, storm surge and river discharge on coastal flood risk: an approach based on 3D fully nested Archimedean copulas, Springer Berlin Heidelberg, 1–32 pp., https://doi.org/10.1007/s12665-022-10719-9, 2023.

Lindström, G., Pers, C., Rosberg, J., Strömqvist, J., and Arheimer, B.: Development and testing of the HYPE (Hydrological Predictions for the Environment) water quality model for different spatial scales, Hydrol. Res., 41, 295–319, https://doi.org/10.2166/nh.2010.007, 2010.

Lucey, J. T. D. and Gallien, T. W.: Characterizing multivariate coastal flooding events in a semi-arid region: The implications of copula choice, sampling, and infrastructure, Nat. Hazards Earth Syst. Sci., 22, 2145–2167, https://doi.org/10.5194/nhess-22-2145-2022, 2022.

Breiman, L.: Random Forests, Mach. Learn., 45, 5–32, https://doi.org/10.1023/A:1010933404324, 2001. ~~Meinshausen, N.: Quantile Regression for Left Truncated Semicompeting Risks Data, J. Mach. Learn. Res., 67, 701-710, https://doi.org/10.1111/j.1541-0420.2010.01521.x, 2011.~~

Moftakhari, H. R., Salvadori, G., AghaKouchak, A., Sanders, B. F., and Matthew, R. A.: Compounding effects of sea level rise and fluvial flooding, Proc. Natl. Acad. Sci. U. S. A., 114, 9785–9790, https://doi.org/10.1073/pnas.1620325114, 2017.

Moftakhari, H., Schubert, J. E., Aghakouchak, A., Matthew, R. A., and Sanders, B. F.: Linking statistical and hydrodynamic modeling for compound flood hazard assessment in tidal channels and estuaries, Adv. Water Resour., 128, 28–38, https://doi.org/10.1016/j.advwatres.2019.04.009, 2019.

Nerger, L., Hiller, W., and Schröter, J.: A comparison of error subspace Kalman filters, Tellus A Dyn. Meteorol. Oceanogr., 57, 715, https://doi.org/10.3402/tellusa.v57i5.14732, 2005.

Olbert, A. I., Moradian, S., Nash, S., Comer, J., Kazmierczak, B., Falconer, R. A., and Hartnett, M.: Combined statistical and hydrodynamic modelling of compound flooding in coastal areas - Methodology and application, J. Hydrol., 620, 129383, https://doi.org/10.1016/j.jhydrol.2023.129383, 2023.

Pawlowicz, R.: M_Map: A mapping package for MATLAB, version 1.4m, [Computer software], available online at www.eoas.ubc.ca/~rich/map.html, 2020.

Pemberton, P., Löptien, U., Hordoir, R., Höglund, A., Schimanke, S., Axell, L., and Haapala, J.: Sea-ice evaluation of NEMO-Nordic 1.0: A NEMO-LIM3.6-based ocean-sea-ice model setup for the North Sea and Baltic Sea, Geosci. Model Dev., 10, 3105–3123, https://doi.org/10.5194/gmd-10-3105-2017, 2017.

Rutgersson, A., Kjellström, E., Haapala, J., Stendel, M., Danilovich, I., Drews, M., Jylhä, K., Kujala, P., Guo Larsén, X., Halsnæs, K., Lehtonen, I., Luomaranta, A., Nilsson, E., Olsson, T., Särkkä, J., Tuomi, L., and Wasmund, N.: Natural Hazards and Extreme Events in the Baltic Sea region, Earth Syst. Dyn. Discuss., 1–80, https://doi.org/10.5194/esd-2021-13, 2021.

Sadegh, M., Moftakhari, H., Gupta, H. V., Ragno, E., Mazdiyasni, O., Sanders, B., Matthew, R., and AghaKouchak, A.: Multihazard Scenarios for Analysis of Compound Extreme Events, Geophys. Res. Lett., 45, 5470–5480, https://doi.org/10.1029/2018GL077317, 2018.

Sadegh, M., Ragno, E., and Aghakouchak, A.: Multivariate Copula Analysis Toolbox (MvCAT): Describing dependence and underlying uncertainty using a Bayesian framework, Eos, Trans. Am. Geophys. Union, 64, 929, https://doi.org/10.1029/eo064i046p00929-04, 2017.

Salvadori, G., Durante, F., Michele, C. De, Bernardi, M., and Petrella, L.: A multivariate copula-based framework for dealing with hazard scenarios and failure probabilities, J. Am. Water Resour. Res., 52, 2–2, https://doi.org/10.1111/j.1752-1688.1969.tb04897.x, 2016.

655 Santos, V. M., Casas-Prat, M., Poschlod, B., Ragno, E., Van Den Hurk, B., Hao, Z., Kalmár, T., Zhu, L., and Najafi, H.: Statistical modelling and climate variability of compound surge and precipitation events in a managed water system: A case study in the Netherlands, Hydrol. Earth Syst. Sci., 25, 3595–3615, https://doi.org/10.5194/hess-25-3595-2021, 2021.

Sentinel-2 cloudless by EOX IT Services GmbH is licensed under a Creative Commons Attribution-NonCommercial-ShareAlike 4.0 International License. The required attribution including the given links is "Sentinel-2 cloudless - 660 https://s2maps.eu by EOX IT Services GmbH (Contains modified Copernicus Sentinel data 2021)". 2021.

Serinaldi, F.: Dismissing return periods!, Stoch. Environ. Res. Risk Assess., 29, 1179–1189, https://doi.org/10.1007/s00477-014-0916-1, 2015.

Strömqvist, J., Arheimer, B., Dahné, J., Donnelly, C., and Lindström, G.: Water and nutrient predictions in ungauged basins: set-up and evaluation of a model at the national scale, Hydrol. Sci. J., 57, 229–247, 665 https://doi.org/10.1080/02626667.2011.637497, 2012.

Tootoonchi, F., Sadegh, M., Haerter, J. O., Räty, O., Grabs, T., and Teutschbein, C.: Copulas for hydroclimatic analysis: A practice-oriented overview, Wiley Interdiscip. Rev. Water, 9, 1–28, https://doi.org/10.1002/wat2.1579, 2022.

Wahl, T., Jain, S., Bender, J., Meyers, S. D., and Luther, M. E.: Increasing risk of compound flooding from storm surge and rainfall for major US cities, Nat. Clim. Chang., 5, 1093–1097, https://doi.org/10.1038/nclimate2736, 2015.

670 Ward, P. J., Couasnon, A., Eilander, D., Haigh, I. D., Hendry, A., Muis, S., Veldkamp, T. I. E., Winsemius, H. C., and Wahl, T.: Dependence between high sea-level and high river discharge increases flood hazard in global deltas and estuaries, Environ. Res. Lett., 13, https://doi.org/10.1088/1748-9326/aad400, 2018.

Wolski, T., Wiśniewski, B., Giza, A., Kowalewska-Kalkowska, H., Boman, H., Grabbi-Kaiv, S., Hammarklint, T., Holfort, J., and Lydeikaite, Ž.: Extreme sea levels at selected stations on the Baltic Sea coast, Oceanologia, 56, 259–290, 675 https://doi.org/10.5697/oc.56-2.259, 2014.

Zscheischler, J., Martius, O., Westra, S., Bevacqua, E., Raymond, C., Horton, R. M., van den Hurk, B., AghaKouchak, A., Jézéquel, A., Mahecha, M. D., Maraun, D., Ramos, A. M., Ridder, N. N., Thiery, W., and Vignotto, E.: A typology of compound weather and climate events, Nat. Rev. Earth Environ., 1, 333–347, https://doi.org/10.1038/s43017-020-0060-z, 2020.